SCIENTIFIC REPORTS

OPEN

SUBJECT AREAS:
ELECTROCATALYSIS
TWO-DIMENSIONAL MATERIALS
FUEL CELLS
POROUS MATERIALS

Received
15 August 2012

Accepted
15 November 2012

Published
7 December 2012

Correspondence and requests for materials should be addressed to Y.D. (yding@sdu.edu.cn) or J.L. (jianguoliu@nju.edu.cn)

# Direct $N_2H_4/H_2O_2$ Fuel Cells Powered by Nanoporous Gold Leaves

Xiuling Yan[1,2], Fanhui Meng[2], Yun Xie[3], Jianguo Liu[3] & Yi Ding[2,4]

[1]Resources and Ecologic Research Institute, School of Chemistry and Bioscience, Yili Normal University, Xinjiang 835000, China, [2]Center for Advanced Energy Materials & Technology Research (AEMT), School of Chemistry and Chemical Engineering, Shandong University, Jinan 250100, China, [3]Eco-materials and Renewable Energy Research Center, Department of Materials Science and Engineering, and National Laboratory of Solid State Microstructures, Nanjing University, Nanjing 210093, China, [4]Shandong Applied Research Center for Gold Technology (Au-SDARC), Yantai 264005, China.

**Dealloyed nanoporous gold leaves (NPGLs) are found to exhibit high electrocatalytic properties toward both hydrazine ($N_2H_4$) oxidation and hydrogen peroxide ($H_2O_2$) reduction. This observation allows the implementation of a direct hydrazine-hydrogen peroxide fuel cell (DHHPFC) based on these novel porous membrane catalysts. The effects of fuel and oxidizer flow rate, concentration and cell temperature on the performance of DHHPFC are systematically investigated. With a loading of ~0.1 mg cm$^{-2}$ Au on each side, an open circuit voltage (OCV) of 1.2 V is obtained at 80°C with a maximum power density 195 mW cm$^{-2}$, which is 22 times higher than that of commercial Pt/C electrocatalyst at the same noble metal loading. NPGLs thus hold great potential as effective and stable electrocatalysts for DHHPFCs.**

The direct liquid $N_2H_4/H_2O_2$ fuel cell (DHHPFC) is known to be a unique power source for air-independent applications under extreme conditions such as outer space and underwater environments. Comparing to fuel cells using oxygen as the oxidizer, the replacement of oxygen by $H_2O_2$ allows much improved reaction kinetics on the cathode as well as higher power density and theoretical open circuit voltage[1,2]. The use of liquid fuel is also beneficial to the construction of more compact and portable power sources. A variety of materials have been designed and investigated as the hydrazine fuel cell catalysts[3–9]. For example, both anion and cation exchange membrane electrode assemblies (MEAs) have been fabricated and studied by Yin and co-workers, using Zr/Ni alloy and carbon supported Pt as anode and cathode catalysts respectively, and a high power density of 84 mW cm$^{-2}$ was observed[5]. Lao and co-workers reported, with a Pt-based anode and an Au/C cathode, a DHHPFC could generate a high power density of 1.02 W cm$^{-2}$ and an open circuit voltage (OCV) of 1.75 V at 80°C with a total catalyst loading of ~10 mg cm$^{-2}$ [9]. Although notable power densities and high OCVs have been achieved, the critical obstacle to the development of fuel cell technology is still the high cost of the catalysts due to excess use of the resource-limited platinum. Furthermore, the current nanoparticle-based electrodes suffer from additional disadvantages, such as structural discontinuity, non-uniform dispersion and serious agglomeration during operation. Therefore, there is still great demand to pursue alternative materials and structures to replace the Pt-based catalysts, while maintaining high enough fuel cell performance and efficiency. In such context, building novel structures facilitating electrons/ions transferring and enhancing the catalytic efficiency of non-platinum catalysts are highly desired in fuel cell community.

Recently, there are rapidly growing interests in Au-based nanotechnology and catalysis[10]. It is quite well known that nanostructural Au can be good electrocatalysts for $N_2H_4$ oxidation[11,12] and $H_2O_2$ reduction[13,14]. This inspired us to develop an Au-based DHHPFC so that Pt can be replaced by this more easily available coinage metal. While a majority of electrocatalysts are based on supported nanoparticles, recently dealloyed porous metals such as nanoporous gold (NPG) were proven to be interesting self-supported nanostructured catalysts and electrocatalysts with some intriguing properties[15–21]. Unlike many other porous materials, dealloyed nanoporous metals possess excellent structural continuity, mechanical rigidity and conductivity, with structural dimension readily tunable from several nanometers to many microns. They have demonstrated great potential for use in heterogeneous catalysis, SERS, actuator, supercapacitors, electrochemical sensors, etc[15–21].

In this paper, we report on the electrocatalytic performance of nanoporous gold leaves (NPGLs)[21] toward $N_2H_4$ oxidation and $H_2O_2$ reduction, with an emphasis on the construction and evaluation of an NPGL-based DHHPFC. Working as both anode and cathode catalysts, NPGLs were found to be able to power a fuel cell with a specific power at least one order of magnitude higher than that of Pt/C under the same testing conditions.

## Results

Similar to the direct borohydride fuel cell (DBFC), DHHPFC is a powerful all-liquid fuel cell that takes advantages of highly active liquid fuel (hydrazine hydrate) and strong liquid oxidizer (hydrogen peroxide). In a DHHPFC, the following electrode reactions occur at the anode and cathode:

Anode: $N_2H_4 + 4OH^- \rightarrow N_2 + 4H_2O + 4e^-$
Cathode: $2H_2O_2 + 4H^+ + 4e^- \rightarrow 4H_2O$
And overall reaction can be written as: $N_2H_4 + 2H_2O_2 \rightarrow N_2 + 4H_2O$

During cell operation, electrons transfer from anode to cathode accompanied with $Na^+$ migration in an opposite direction through a Nafion membrane (Figure 1). Considering the working mechanism, the overall reaction can also be understood as $N_2H_4 + 2NaOH + 2H_2O_2 + H_2SO_4 \rightarrow N_2 + Na_2SO_4 + 6H_2O$. This configuration is similar to the direct borohydride/hydrogen peroxide fuel cell that uses concentrated NaOH as the anolyte and $H_3PO_4$ as the catholyte[22,23]. An ideal electrocatalyst for this type of fuel cells should have a high surface area open framework (nanoporosity) to allow fast ion/molecule diffusion, and highly active surfaces to initiate the electrocatalytic reactions and is intrinsically highly conductive for electron transportation[17,24]. NPGL happens to be such a material that fulfills all these key structural properties.

To evaluate the catalytic activities of NPGL, cyclic voltammetric (CV) tests of various samples toward $N_2H_4$ and $H_2O_2$ were conducted. Three NPGL samples were prepared and compared by dealloying 12-carat white gold leaves[21] in concentrated nitric acid for 15, 30, 60 minutes, which were denoted as NPGL15, NPGL30 and NPGL60, respectively. Figure 2A shows CV plots of these NPGL samples in 0.01 M NaOH containing 10 mM $N_2H_4$. In the range of $-0.6 \sim -0.1$ V *vs.* SCE, the anode peaks for $N_2H_4$ oxidation on these three electrodes locate around $-0.45$, $-0.41$ and $-0.34$ V, respectively, and a slight decrease in current is seen upon increase in dealloying time. These results are generally consistent with the previous report that shorter etching time often leads to smaller pore size and higher activity[25]. For NPGL30, the oxidation peak current density was up to 10.5 mA $cm^{-2}$, with a peak potential at about $-0.41$ V, which was 11 times higher and 480 mV more negative than that on a bulk Au electrode (inset of Figure 2A, 0.9 mA $cm^{-2}$ at 0.07 V). In comparison, no noticeable current peak can be observed for bare GCE (curve d), indicating that NPGL is the major contributor to $N_2H_4$ oxidation.

Figure 2B shows the CVs of NPGLs in 10 mM $H_2O_2$. A quite similar trend can be found for $H_2O_2$ reduction for NPGL samples of different type. Accompanying the decrease in pore size, catalytic activity increases. For NPGL30, the onset reduction potential was about 95 mV, which was nearly 100 mV more positive than that on a bulk Au electrode ($\sim$0 V, inset of Figure 2B), suggesting that NPGL30 can efficiently catalyze the reduction reaction. Again, there is negligible activity for GCE (curve d) toward this reaction.

For electrochemical redox reactions of $N_2H_4$ and $H_2O_2$, NPGL15 shows the highest catalytic activity in both cases. However, considering that there is appreciable amount of residual Ag (4.88%, Table 1) in the NPGL15 sample, which might get lost during electrochemical and fuel cell testing and thus influence the evaluation of sample performance and stability[26], NPGL30 was selected instead to assemble MEAs for fuel cell tests as discussed below.

## Discussion

In view of the high catalytic activities of NPGL, MEAs for DHHPFCs were constructed by sandwiching a Nafion 115 membrane with two pieces of NPGL30 on each side (see Methods for details). As observed in Figure 2C, 100 nm thick NPGLs can be readily attached onto both sides of the membrane without breakage. Its excellent mechanical rigidity and structural continuity are also beneficial to the decrease of mass and electron transferring resistance in discharging processes. Figure 2D depicts a single cell within which such an NPGL-based MEA was assembled, and the device performance was investigated under various conditions such as fuel flow rate, fuel concentration, and cell temperatures. The durability of this interesting electrocatalyst was also evaluated.

As illustrated in a scheme shown in Figure 1, $Na^+$ is the main charge carrier during DHHPFC operation. To prove this critical point, flame atomic absorption spectroscopy (FAAS) measurements were first carried out and the results were collected in Table 2. It shows that the concentration of $Na^+$ in the catholyte increases dramatically with the increase of discharging time, which implies that $Na^+$ has effectively transported to the cathode side and is indeed the main charge carrier during DHHPFC operation.

Considering the distinct electrolytes on each side of Nafion membrane, possible acid-base neutralization might occur which would lead to heat production and fast deterioration of the entire system. However, pH and temperature measurements showed that our system was rather stable. From Table 2, there is only slight variation of pH values during 300 min operation, which could be ascribed to the consumption of the respective ions on the electrodes. And the temperature variation of below 0.5°C proves that the mixing of $OH^-$ or $H^+$ did not occur in this system, a further evidence for the stability of the DHHPFC.

Considering the varying activity with pH and to optimize the fuel cell performance, experiments were conducted at various concentrations of NaOH and $H_2SO_4$. As observed in Table 3, in the absence of

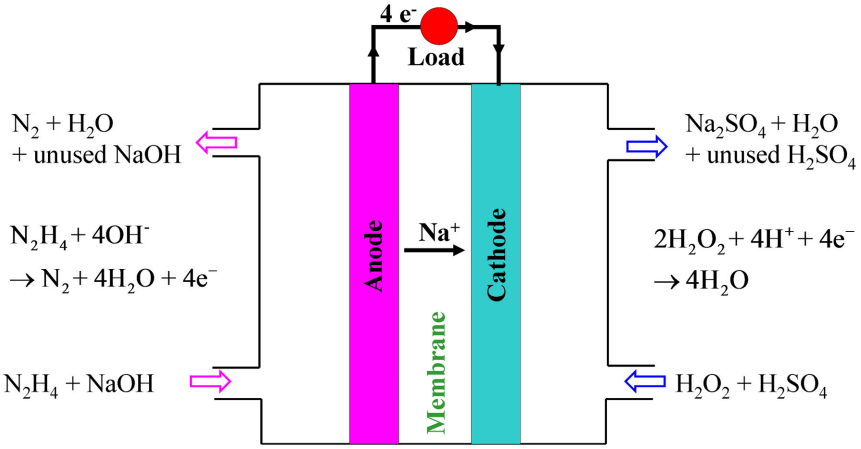


**Figure 1 | Electrode reactions and working mechanism of the DHHPFC.**

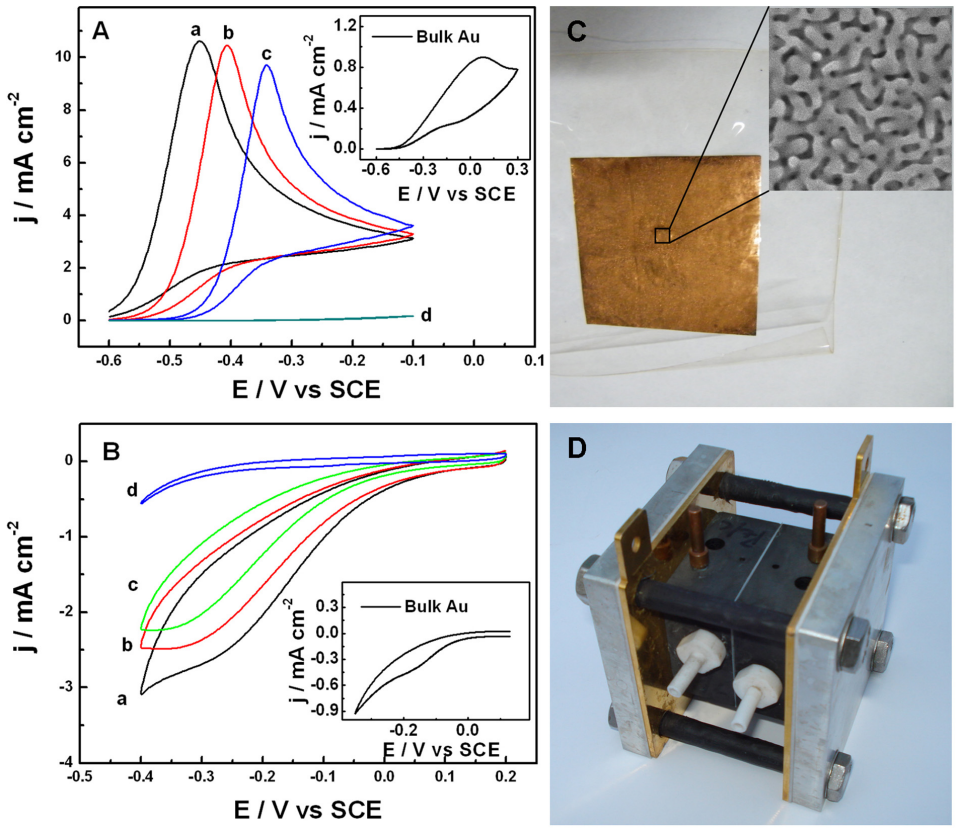


**Figure 2 | Cyclic voltammetry of NPGL15 (a), NPGL30 (b), NPGL60 (c), and GCE (d) in (A) 0.01 M NaOH containing 10 mM $N_2H_4$, and in (B) 0.5 M $H_2SO_4$ containing 10 mM $H_2O_2$.** Scan rate: 50 mV $s^{-1}$. The insets show the respective voltammograms of bulk Au electrode for these two reactions. Digital photographs of (C) a NPGL-based MEA and (D) a DHHPFC single cell.

fuel and oxidizer, the OCV values increase as the concentration of $H_2SO_4$ and/or NaOH gets higher. For example, the cell could demonstrate a voltage of 0.489 V when 4 M NaOH and 0.5 M $H_2SO_4$ were separated by the membrane. However, the cell could not discharge due to the lack of an effective and continuous redox reaction, even at a very small current density of 1 mA $cm^{-2}$. In comparison, adding liquid fuel and oxidizer to each side would lead to dramatic increase of both OCV and the current output. It is noted that NaOH addition in anolyte and $H_2SO_4$ addition in catholyte are beneficial to improvement of the DHHPFC performance, which is in agreement with literature report of Lao et al[9]. According to the optimization of cell performance, 4 M NaOH and 0.5 M $H_2SO_4$ were selected as the appropriate electrolytes.

To optimize the fuel concentrations, the experimental temperature was controlled at 60°C , and the anode and the cathode flow rates were set at 1.4 and 4.2 mL $min^{-1}$, respectively. As shown in Figure 3A, with a fixed $H_2O_2$ concentration of 20 wt.%, the OCVs locate at around 1.06 V regardless of the varying of the $N_2H_4$ concentration. However, their MPD sees evident improvement from 50 to 98.2 mW $cm^{-2}$ as the concentration of $N_2H_4$ increased from 5 to 10 wt.%. Interestingly, when the concentration of $N_2H_4$ further increased to 20 wt.%, the MPD would decrease to 82.1 mW $cm^{-2}$.

As observed in Figure 3B, both the OCV and MPD underwent dramatic changes in value with increase in concentration of $H_2O_2$ from 5 to 20 wt.% when the anode concentration of $N_2H_4$ was fixed at 10 wt.%. Within this concentration range, the cell OCV and MPD increased from 0.84 V and 36.1 mW $cm^{-2}$ to 1.08 V and 98.2 mW $cm^{-2}$.

Two factors simultaneously influence the cell performance when the $N_2H_4$ concentration changes. On one hand, fuel transfer rate will increase due to the higher concentration gradient of $N_2H_4$, leading to higher power density. On the other hand, the amount of fuel crossover and the degree of $N_2H_4$ hydrolysis may become serious, which will reduce cell performance. Therefore, an optimized fuel concentration for the MEAs used in this work should be around 10 wt.%. On the cathode side, the rate-determining step should be the transfer of $H_2O_2$ since no decay of the DHHPFC was found even when the concentration of $H_2O_2$ increased to 20 wt.%. In terms of cell performance optimization, 10 wt.% $N_2H_4$ and 20 wt.% $H_2O_2$ were selected as the optimal concentration in the following tests.

Table 1 | EDS data of NPGL samples before and after fuel cell tests

| | Wt.% | | | |
|---|---|---|---|---|
| Element | NPGL15[a] | NPGL30[b] | NPGL30-1[c] | NPGL30-2[d] |
| Au | 95.12 | 98.31 | 98.45 | 99.34 |
| Ag | 4.88 | 1.69 | 1.55 | 0.66 |

[a,b]fresh NPGL before fuel cell test.
[c]NPGL at the anode after fuel cell test.
[d]NPGL at the cathode after fuel cell test.

Table 2 | pH value, temperature and concentration of $Na^+$ in the catholyte at different discharging stages

| Discharging time | pH | | Temperature/°C | | $Na^+$/mg $mL^{-1}$ |
|---|---|---|---|---|---|
| | Anode | Cathode | Anode | Cathode | |
| 30 min | 13.68 | 0.82 | 24.6 | 24.5 | 1.21 |
| 60 min | 13.56 | 1.02 | 24.6 | 24.5 | 2.13 |
| 300 min | 13.23 | 1.21 | 24.9 | 24.8 | 8.69 |

Table 3 | Performance of DHHPFC with various concentrations of electrolyte

| Anolyte | Catholyte | OCV/V | MPD/mW cm$^{-2}$ |
|---|---|---|---|
| 4 M NaOH | 0.05 M $H_2SO_4$ | 0.249 | — |
| 4 M NaOH | 0.5 M $H_2SO_4$ | 0.489 | — |
| 4 M NaOH | 1 M $H_2SO_4$ | 0.665 | — |
| 0.4 M NaOH | 0.5 M $H_2SO_4$ | 0.334 | — |
| 0.04 M NaOH | 0.5 M $H_2SO_4$ | 0.188 | — |
| 0.04 M NaOH+10% $N_2H_4$ | 0.5 M $H_2SO_4$+20% $H_2O_2$ | 0.531 | 16.44 |
| 0.4 M NaOH+10% $N_2H_4$ | 0.5 M $H_2SO_4$+20% $H_2O_2$ | 0.750 | 23.08 |
| 4 M NaOH+10% $N_2H_4$ | 0.5 M $H_2SO_4$+20% $H_2O_2$ | 1.025 | 99.47 |
| 4 M NaOH+10% $N_2H_4$ | 0.05 M $H_2SO_4$+20% $H_2O_2$ | 0.630 | 63.63 |

In order to study the influence of fuel flow rate on the cell performance, the experimental temperature was kept at 60°C and the concentrations of both anode and cathode electrolyte solutions were maintained at 10 wt.%. The current-voltage and current-power polarization curves of a DHHPFC under different flow rates were then investigated. As shown in Figure 3C, when the $H_2O_2$ flow rate was set at 4.2 mL min$^{-1}$, by varying the $N_2H_4$ flow rate from 0.7 to 1.4 mL min$^{-1}$ there was very little change for the OCV and maximum power density (MPD). When the anode flow rate increased to 2.8 mL min$^{-1}$, the OCV decreased ~30 mV, resulting in a concomitant 4 mW cm$^{-2}$ decrease in MPD. In Figure 3D, when the $N_2H_4$ flow rate was maintained at 1.4 mL min$^{-1}$, by varying the $H_2O_2$ flow rate from 2.1 to 6.3 mL min$^{-1}$, the OCV remained nearly unchanged while the MPD showed a gradual increase from 44.5, 61.8 to 64 mW cm$^{-2}$.

As shown in Figure 3C, the MPD slightly decreased upon the increase of the anode flow rate. This could be attributed to an increase of $N_2H_4$ permeation at the high flow rate, which led to the decline of the overall performance. Therefore, the anode flow rate of 1.4 mL min$^{-1}$ was chosen as an appropriate value in the following tests.

It was noted that the decomposition of $H_2O_2$ on the cathode side was quite severe as compared with that of $N_2H_4$ on the anode. And the released oxygen bubbles may block the transfer of $H_2O_2$ molecules to the catalytic sites of NPGLs. The larger flow rate of $H_2O_2$ is therefore beneficial to flush away these obstructing oxygen bubbles on the catalyst surface, which in turn results in a positive effect on the cell performance. As the $H_2O_2$ flow rate increased to over 4.2 mL min$^{-1}$, the voltage gain became negligible. Therefore, 4.2 mL min$^{-1}$ was selected as an appropriate cathode flow rate in the following experiments.

While temperature is an important factor influencing the device performance, tests were carried out at 40, 60 and 80°C. Figure 4A presents typical polarization curves of DHHPFCs at various cell temperatures. It can be seen that the cell performance can be significantly improved at higher temperature, generating the respective

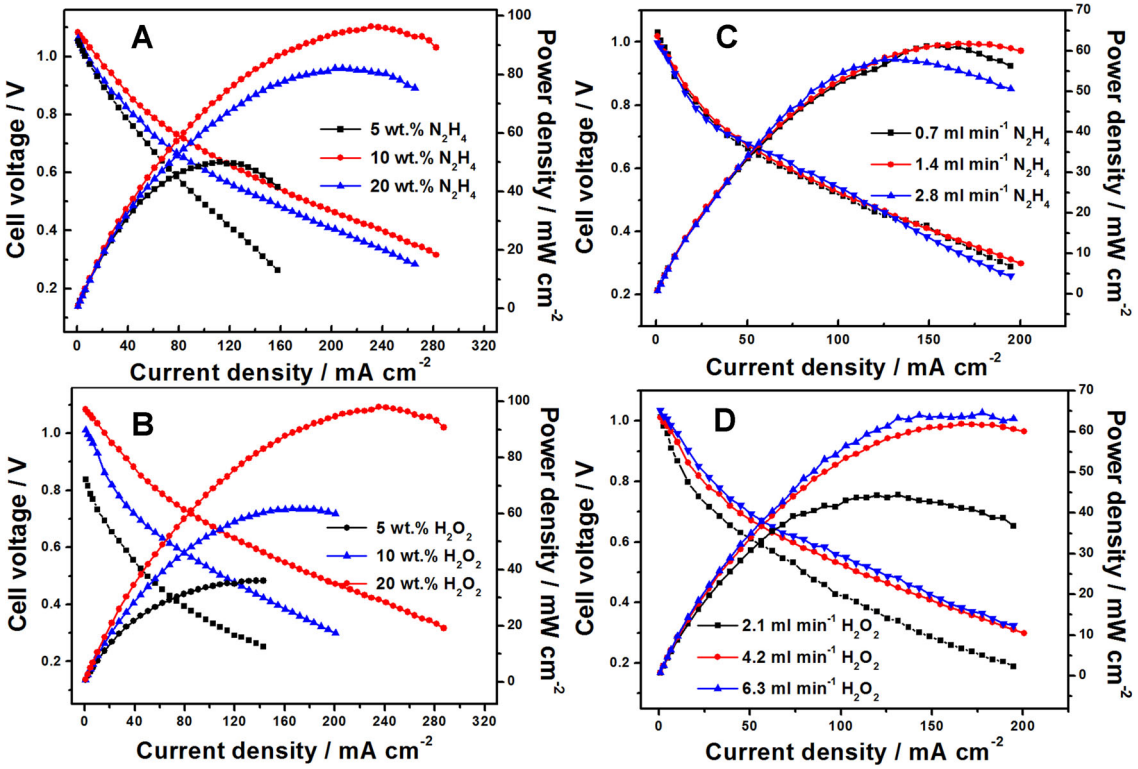


**Figure 3 | Performance of the DHHPFC under various electrolyte conditions with NPGL30 as the catalyst at 60°C.** (A) Dependence of the $N_2H_4$ concentration, the $H_2O_2$ concentration was fixed at 20 wt.%; (B): Dependence of the $H_2O_2$ concentration, $N_2H_4$ concentration was fixed at 10 wt.%. The flow rates of the fuel and oxidizer were 1.4 and 4.2 mL min$^{-1}$, respectively. (C) Dependence of the $N_2H_4$ flow rate as the cathode flow rate was fixed at 4.2 mL min$^{-1}$; (D) Dependence of the $H_2O_2$ flow rate as the anode flow rate was fixed at 1.4 mL min$^{-1}$. The concentrations of $N_2H_4$ and $H_2O_2$ were 10 wt.%.

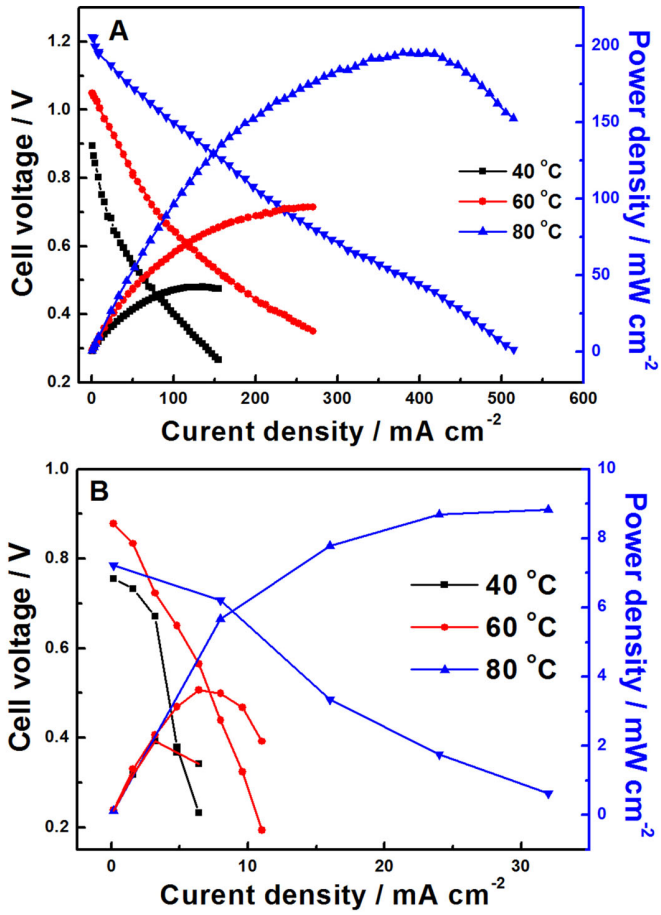


**Figure 4 | Performance of DHHPFC at various temperatures with NPGL30 (A) and Pt/C (B) as the catalysts for both anode and cathode, 4 M NaOH + 10 wt.% $N_2H_4$ as anolyte and 0.5 M $H_2SO_4$ + 20 wt.% $H_2O_2$ as catholyte.** The flow rates of the anolyte and catholyte were 1.4 and 4.2 mL $min^{-1}$, respectively.

MPD values at around 42.5, 94.5, and 195.4 mW $cm^{-2}$. Accordingly, their OCVs were 0.89, 1.05 and 1.21 V, respectively. The increase in cell performance at higher temperature may be attributed to the enhanced kinetics of both the anodic and cathodic reactions and higher conductivity of the electrolyte[27,28].

The experimentally observed 1.21 V is still much lower than the theoretical OCV of DHHPFC (2.13 V)[9]. This large deviation was mainly due to the high over-potential, which can in part be reduced by the elevation of cell temperature. This also explains the higher OCV and better performance obtained at higher temperature. On the other hand, with the 125 microns thick Nafion membrane, crossover of $N_2H_4$ and $H_2O_2$ is possible, which would reduce the cell performance. Indeed, by effectively separating the anode and cathode in a cell configuration using two Nafion membranes, an even higher OCV of 1.45 V was observed. However, discharge performance was significantly lower due to the high cell resistance.

Because the Au loading for NPGL is around 0.1 mg $cm^{-2}$ on each side, the highest performance observed at 80°C can thus be calculated to give a specific power of 975 mW $mg^{-1}$. The power density of 195.4 mW $cm^{-2}$ is twice higher than that of binary alloy catalysts[5], and if the catalyst efficiency is counted, the specific power is nearly one order of magnitude higher than the mixed Pt-based electrode[9]. For comparison purpose, we also tested a DHHPFC with the same loading of platinum (0.1 mg $cm^{-2}$) on each side by using the commercial 60 wt.% Pt/C catalyst (Johnson Matthey, UK). From Figure 4B, the MPD was only 8.8 mW $cm^{-2}$ at 80°C, which is nearly 22 times lower than that of NPGL. Considering the comparatively larger world resources of Au compared to Pt, our results show the potential of using Au nanostructures for certain applications, such as DHHPFC.

Stability of the DHHPFC was evaluated by discharging at 150 mA $cm^{-2}$ for 6 hours a day within three consecutive days at 60°C. The result is shown in Figure 5, where the fluctuation of cell voltage was due to the oxygen generated from the cathode by $H_2O_2$ decomposition or the hydrogen generated from the anode by $N_2H_4$ hydrolysis. The generated gas bubbles may accumulate on the surface of electrodes and block the transferring of $N_2H_4$ or $H_2O_2$ solution, which results in instant performance loss. However, the cell voltage can be quickly restored to its normal discharge voltage as shown in Figure 5. During the first day of testing, the initial cell potential was 0.89 V, and it decreased to 0.87 V after 6 hours continuous discharging. The reason for performance deterioration may be related to the accumulation of some reaction intermediates onto the surfaces of NPGL catalyst rather than the irreversible structural change of the catalyst itself. This is supported by a totally recovered cell performance in the following two days (Figure 5). Although the long term durability of our catalysts and DHHPFCs needs further exploration, our preliminary results showed that the catalytic activity of NPGL30 toward $N_2H_4$ oxidation and $H_2O_2$ reduction was relatively stable in DHHPFCs.

To confirm the catalyst stability, the SEM images of NPGL before and after fuel cell tests are presented in Figure 6. From the surface and cross-sectional SEM images shown in Figure 6A&B, it can be seen that NPGL30 has a 30 nm pore size structure across the whole thickness of about 100 nm. After the fuel cell tests, the sample was carefully detached from the MEA and characterized by SEM. Figure 6C&D illustrate the morphology of NPGL30 on the anode and cathode, respectively. Compared to the fresh samples, there is only a slight increase in pore size to around 35 nm. We analyzed the compositional information with Energy Dispersive X-ray Spectroscopy (EDS) (Table 1), and found the changes of Ag content for the anode and cathode were quite different upon fuel cell test. The silver content of NPGL30 on the cathode decreased more obviously than that on the anode. This may be attributed to the formation of $Ag_2O$ during a positive potential sweep in $H_2O_2$[26]. However, Ag content did not greatly change at the anode, indicating that Ag is rather stable at negative potentials in the presence of $N_2H_4$.

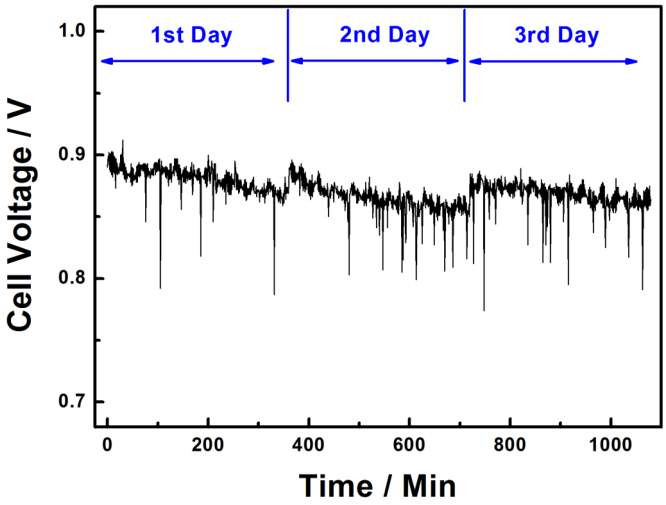


**Figure 5 | Durability test of the DHHPFC within three consecutive days with NPGL30 as the catalyst at 60°C.** The flow rates of the anolyte and catholyte were 1.4 and 4.2 mL $min^{-1}$, respectively.

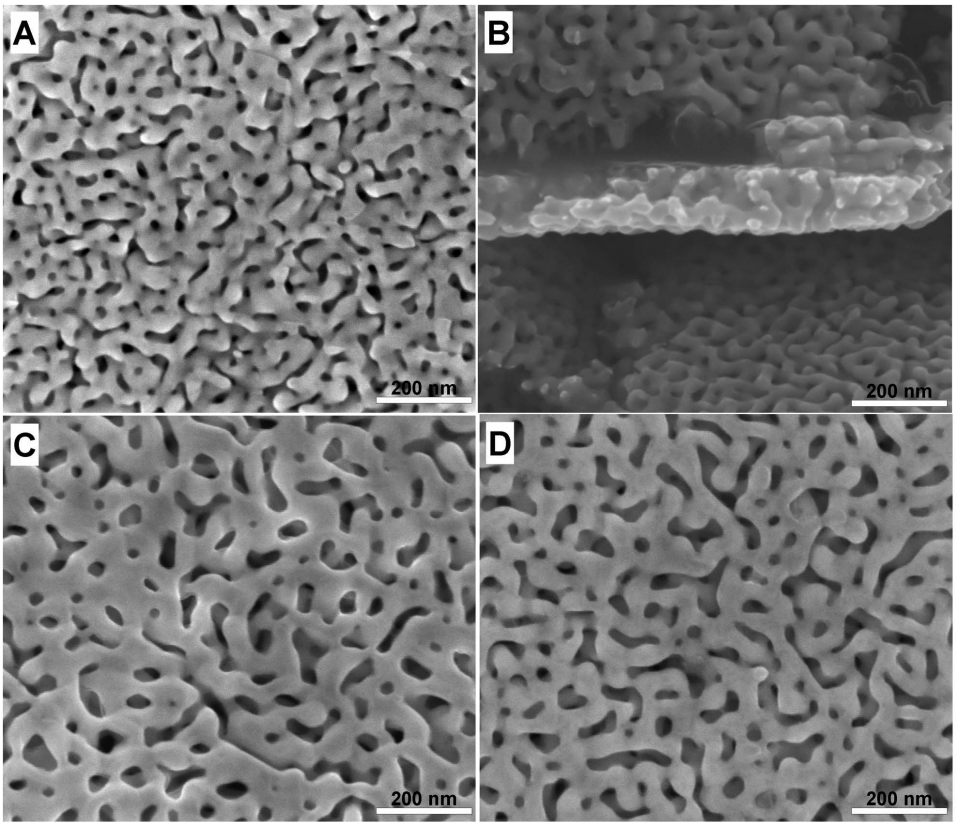


**Figure 6 | Scanning electron microscopy (SEM) images of NPGL30.** Surface (A) and cross-sectional (B) micro-morphology of a fresh sample; Anode (C) and Cathode (D) surface micro-morphology after fuel cell tests.

In summary, we demonstrated that dealloyed nanoporous gold in a free-standing leaf form can function as novel electrocatalysts on both anode and cathode in a hydrazine/hydrogen peroxide fuel cell. This is due to NPGL's intrinsically high electrocatalytic activities toward $N_2H_4$ oxidation and $H_2O_2$ reduction, a behavior not readily seen on planar Au electrode. Under optimized conditions, a high power density of 195.4 mW $cm^{-2}$ can be realized on an MEA using 0.1 mg Au on each electrode, generating an impressive specific power of 975 mW $mg^{-1}$. Considering there are a big selection of nanoporous metals (NPMs) including alloys[29] and less precious metals[30] and these new materials all possess tunable porosity and tailored surface chemistry[31], NPMs might become a new generation nanoparticle-free catalysts or electrodes for a wide variety of energy and environmental technologies.

## Methods

**Preparation and characterization of NPGL.** NPGLs with a thickness of 100 nm were prepared by etching 12-carat white gold leaves ($Au_{50}Ag_{50}$ wt.%, Sepp Leaf Products, USA) at 303 K in concentrated nitric acid (~65%) for 15, 30, 60 minutes, which were denoted as NPGL15, NPGL30 and NPGL60, respectively. The morphology and composition were characterized by scanning electron microscopy (SEM) on an FEI NOVA NanoSEM 230 equipped with Energy Dispersive X-ray Spectroscopy.

**Electrochemical tests.** To fix NPGL onto the surface of glassy carbon electrodes (GCE), NPGL was first transferred into a beaker containing 500 mL water with a glass slide. A polished GCE was then dipped into the water underneath to allow the entire conducting GC circle covered by NPGL on top. The NPGL-coated GCE was then carefully taken out of the water, air-dried, trimmed and finally fixed by Nafion solution. The electrochemical measurements of NPGLs were carried out on a potentiostatic (CHI760C, China) in a three-electrode configuration with a platinum foil as the counter electrode and a saturated calomel electrode (SCE) as the reference electrode. Supporting electrolyte was deoxygenated by bubbling high purity nitrogen for at least 20 minutes before each experiment.

**Fuel cell assemble and tests.** Nafion 115 membrane was used as the solid electrolyte. In order to remove organic contaminants and heavy metal ions, the membrane was treated with 3 wt.% $H_2O_2$ solution, ultra pure water, 0.5 M $H_2SO_4$ and ultra pure water in turn at 80°C for 1 h.

The NPGL-based MEA was made by first lifting NPGL onto a carbon paper (TGP-H-060, Toray, Japan), and after drying they were hot-pressed onto both sides of a Nafion 115 membrane at 110°C and 0.5 MPa for 3 minutes.

Pt/C (60 wt.%, Johnson Matthey, UK) catalysts were dispersed in ethanol in ultrasonic bath for 10 min before mixing with 5 wt.% Nafion solution. The ink was precisely sprayed on gas-diffusion layer by ultrasonic spraying coating system (Exacta. Coat, Sono-Tek, USA) with Pt loading of 0.1 mg $cm^{-2}$. The MEA was obtained by hot-pressing onto both sides of a pre-treated Nafion 115 membrane at 140°C and 0.5 MPa for 3 min.

To maintain a stable operating condition, on the anode side the fuel was mixed with 4 M NaOH, while on the cathode side 0.5 M $H_2SO_4$ was used in the electrolyte. $N_2H_4$ and $H_2O_2$ were pumped to the anode and cathode at desired concentration and flow rate by individual peristaltic pumps and silicone tubes. The cell temperature was controlled via a temperature controller and monitored by thermocouples buried in the graphite blocks. The steady state polarization curves were recorded by an automatic Electric Load (PLZ 70UA, Japan).

Flame atomic absorption spectroscopy (FAAS 3510, China) measurements were performed in order to prove that $Na^+$ is the main charge carrier during DHHPFC operation. The pH values of anolyte and catholyte were collected with a Sartorius PB-10 pH meter.

1. Gu, L., Luo, N. & Miley, G. H. Cathode electrocatalyst selection and deposition for a direct borohydride/hydrogen peroxide fuel cell. *J. Power Sources* **173**, 77–85 (2007).
2. Cao, D., Chen, D., Lan, J. & Wang, G. An alkaline direct $NaBH_4$-$H_2O_2$ fuel cell with high power density. *J. Power Sources* **190**, 346–350 (2009).
3. Serov, A. & Kwak, C. Direct hydrazine fuel cells: A review. *Appl. Catal. B: Environ.* **98**, 1–9 (2010).
4. Yamada, K. *et al.* Potential application of anion-exchange membrane for hydrazine fuel cell electrolyte. *Electrochem. Commun.* **5**, 892–896 (2003).
5. Yin, W., Li, Z., Zhu, J. & Qin, H. Effects of NaOH addition on performance of the direct hydrazine fuel cell. *J. Power Sources* **182**, 520–523 (2008).
6. Asazawa, K. *et al.* A platinum-free zero-carbon-emission easy fuelling direct hydrazine fuel cell for vehicles. *Angew. Chem. Int. Ed.* **46**, 8024–8027 (2007).

7. Gu, H. *et al.* Solid-oxide fuel cell operated on in situ catalytic decomposition products of liquid hydrazine. *J. Power Sources* **177**, 323–329 (2008).
8. Yamada, K. *et al.* Investigation of PEM type direct hydrazine fuel cell. *J. Power Sources* **115**, 236–242 (2003).
9. Lao, S. *et al.* A development of direct hydrazine/hydrogen peroxide fuel cell. *J. Power Sources* **195**, 4135–4138 (2010).
10. Haruta, M. Catalysis-Gold rush. *Nature* **437**, 1098–1099 (2005).
11. Li, J. & Lin, X. Electrocatalytic oxidation of hydrazine and hydroxylamine at gold nanoparticle-polypyrrole nanowire modified glassy carbon electrode. *Sensor. Actuat. B-Chem.* **126**, 527–535 (2007).
12. Jena, B. K. & Raj, C. R. Ultrasensitive nanostructured platform for the electrochemical sensing of hydrazine. *J. Phys. Chem. C* **111**, 6228–6232 (2007).
13. Zeis, R., Lei, T., Sieradzki, K., Snyder, J. & Erlebacher, J. Catalytic reduction of oxygen and hydrogen peroxide by nanoporous gold. *J. Catal.* **253**, 132–138 (2008).
14. Meng, F., Yan, X., Liu, J., Gu, J. & Zou, Z. Nanoporous gold as non-enzymatic sensor for hydrogen peroxide. *Electrochim. Acta* **56**, 4657–4662 (2011).
15. Ding, Y. & Chen, M. Nanoporous metals for catalytic and optical applications. *MRS Bull.* **34**, 569–576 (2009).
16. Fujita, T. *et al.* Atomic origins of the high catalytic activity of nanoporous gold. *Nat. Mater.* **11**, 775–780 (2012).
17. Nagle, L. C. & Rohan, J. F. Nanoporous Gold anode catalyst for Direct Borohydride Fuel Cell. *Int. J. Hydrogen Energ.* **36**, 10319–10326 (2011).
18. Nagle, L. C. & Rohan, J. F. Nanoporous Gold Catalyst for Direct Ammonia Borane Fuel Cell. *J. Electrochem. Soc.* **158**, B5772–B5778 (2011).
19. Yan, X. *et al.* Effective and rapid electrochemical detection of hydrazine by nanoporous gold. *J. Electroanal. Chem.* **661**, 44–48 (2011).
20. Zhang, Z. *et al.* Generalized Fabrication of Nanoporous Metals (Au, Pd, Pt, Ag, and Cu) through Chemical Dealloying. *J. Phys. Chem. C* **113**, 12629–12636 (2009).
21. Ding, Y., Kim, Y. J. & Erlebacher, J. Nanoporous gold leaf: Ancient technology/advanced material. *Adv. Mater.* **16**, 1897–1900 (2004).
22. Miley, G. H. *et al.* Direct $NaBH_4/H_2O_2$ fuel cells. *J. Power Sources* **165**, 509–516 (2007).
23. Byrd, E. D. & Miley, G. H. Simulation studies of the membrane exchange assembly of an all-liquid, proton exchange membrane fuel cell. *J. Power Sources* **176**, 222–228 (2008).
24. Zeis, R., Mathur, A., Fritz, G., Lee, J. & Erlebacher, J. Platinum-plated nanoporous gold: An efficient, low Pt loading electrocatalyst for PEM fuel cells. *J. Power Sources* **165**, 65–72 (2007).
25. Zhang, J., Liu, P., Ma, H. & Ding, Y. Nanostructured porous gold for methanol electro-oxidation. *J. Phys. Chem. C* **111**, 10382–10388 (2007).
26. Doblhofer, K. *et al.* Autocatalysis by the intermediate surface hydroxide formed during hydrogen peroxide reduction on silver electrodes. *Surf. Sci.* **603**, 1900–1903 (2009).
27. Choudhury, N. A., Raman, R. K., Sampath, S. & Shukla, A. K. An alkaline direct borohydride fuel cell with hydrogen peroxide as oxidant. *J. Power Sources* **143**, 1–8 (2005).
28. Cao, D., Gao, Y., Wang, G., Miao, R. & Liu, Y. A direct $NaBH_4$–$H_2O_2$ fuel cell using Ni foam supported Au nanoparticles as electrodes. *Int. J. Hydrogen energy* **35**, 807–813 (2010).
29. Xu, C. *et al.* Dealloying to nanoporous Au/Pt alloys and their structure sensitive electrocatalytic properties. *Phys. Chem. Chem. Phys.* **12**, 239–246 (2010).
30. Xu, C. *et al.* Nanotubular mesoporous bimetallic nanostructures with enhanced electrocatalytic performance. *Adv. Mater.* **21**, 2165–2169 (2009).
31. Li, Y. Y. & Ding, Y. Porous AgCl/Ag nanocomposites with enhanced visible light photocatalytic properties. *J. Phys. Chem. C* **114**, 3175–3179 (2010).


## Acknowledgements

This work was supported by the National Basic Research Program of China (2012CB932800) and the National Science Foundation of China (51171092, 20906045, 90923011). Y. D. is a Tai-Shan Scholar supported by the Independent Innovation Foundation of Shandong University (IIFSDU).

## Author contributions

Y.D. and J.L. designed this research; X.Y. carried out the experiments and analyzed the data; F.M. and Y.X. contributed to the experimental testing; X.Y. and Y.D. wrote the paper.

## Additional information

**Competing financial interests:** The authors declare no competing financial interests.



**How to cite this article:** Yan, X., Meng, F., Xie, Y., Liu, J. & Ding, Y. Direct $N_2H_4/H_2O_2$ Fuel Cells Powered by Nanoporous Gold Leaves. *Sci. Rep.* **2**, 941; DOI:10.1038/srep00941 (2012).